Prediction of static properties of LPBF AlSi10Mg samples post-treated by Friction Stir Processing or thermal treatments

[1] Tran Hoang Son, [1] Chantal Bouffioux, [2] Olivier Dedry, [2] Jocelyn Delahaye, [1] Seifallah Fetni, [2] Anne Mertens, [1] Laurent Duchêne and [1] Anne Marie Habraken

[1] Materials and Solid Mechanics, University of Liège, Liège, Belgium

[2] Metallic Materials Science, University of Liège, Liège, Belgium

18th European Mechanics of Materials Conference

Oxford 4th April 2022

Experimental context

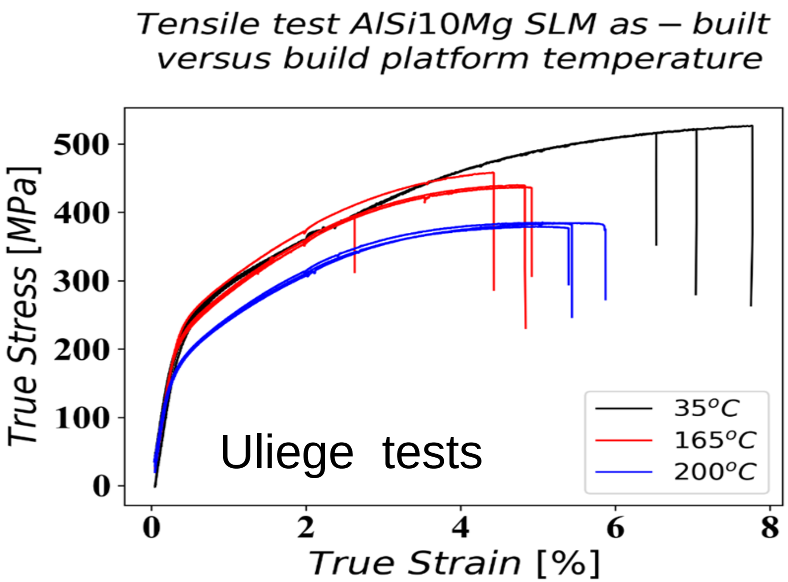

J.G. Santos Macías Acta Materialia 201 (2020)

As built microstructure AB

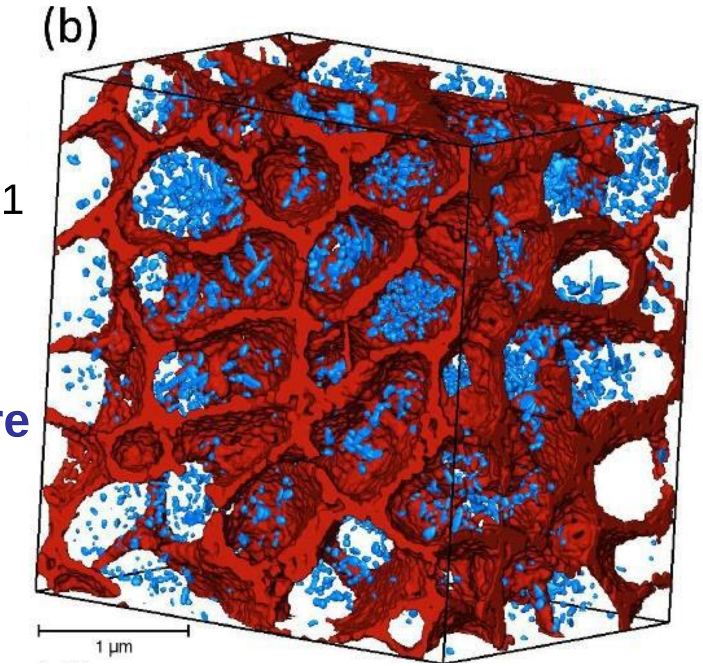

Post treatment effects (thermal treatment TT or Friction Stir Processing FSP)

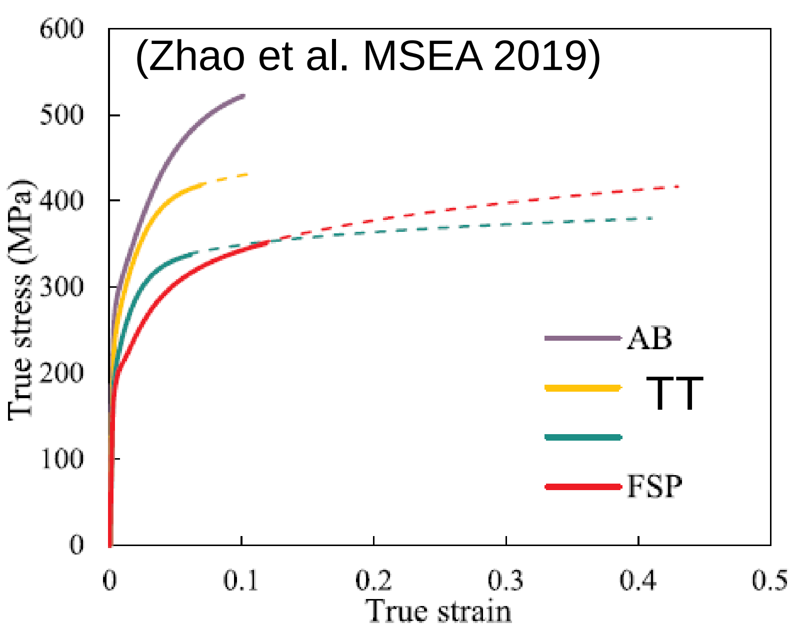

+ DSC, SEM, DRX
→ Microstructure **Evolution AB**

Nano indentation
→ **Local Mechanical properties**

Microstructure AB +TT

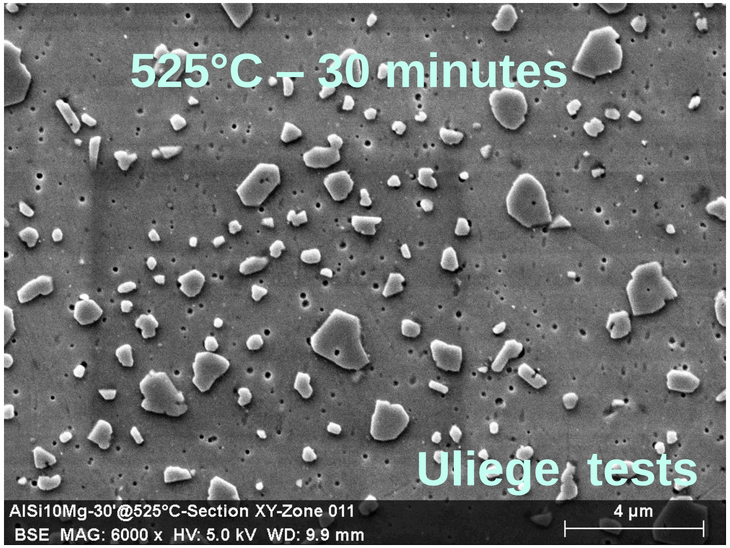

Toward Numerical Material Design

1. **Microstructure Prediction & Properties**

Finite Element Model of LPBF FEM

\+

AB Microstructure characterization

Conduction, Capacity and Density (see ESAFORM 2021 Delahaye,Orbi Presentation)

Yield limit σ_y

Initial temperature history
→ out of balance microstructure
“ 5 layers simulations ”

→ internal heat treatment when the whole sample is manufactured at 165°C or 200°C

PHASE FIELD model PF

Thermo physical properties

Mechanical properties

Predicted Microstructure (validated by charact.)

AB & internal TT (35°C, 165°C, 200°C)
AB & TT post treatment
AB 1st run DSC
AB 2nd run DSC

AB & FSP post treatment

\+

Analytical tools

DSC Differential Scanning Calorimetry
FSP Friction Stir Processing

Toward Numerical Material Design

2. Microstructure Design through RVE

OM, SEM or results of PF → Microstructure EF meshes

\+

Representative Volume Element RVE

\+

Nanoindentation for local material properties

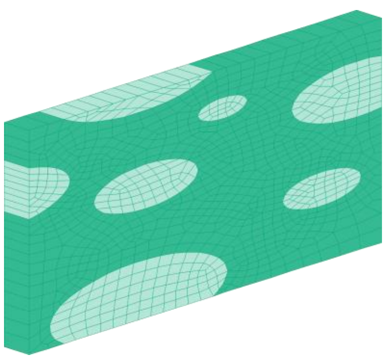

AB & internal TT
(35°c 165°c 200°C)
AB & TT post treatment
AB & FSP post treatment
AB 1st runt DSC
AB 2nd run DSC

→

σ-ε curve
Damage mechanism
Static
Fatigue

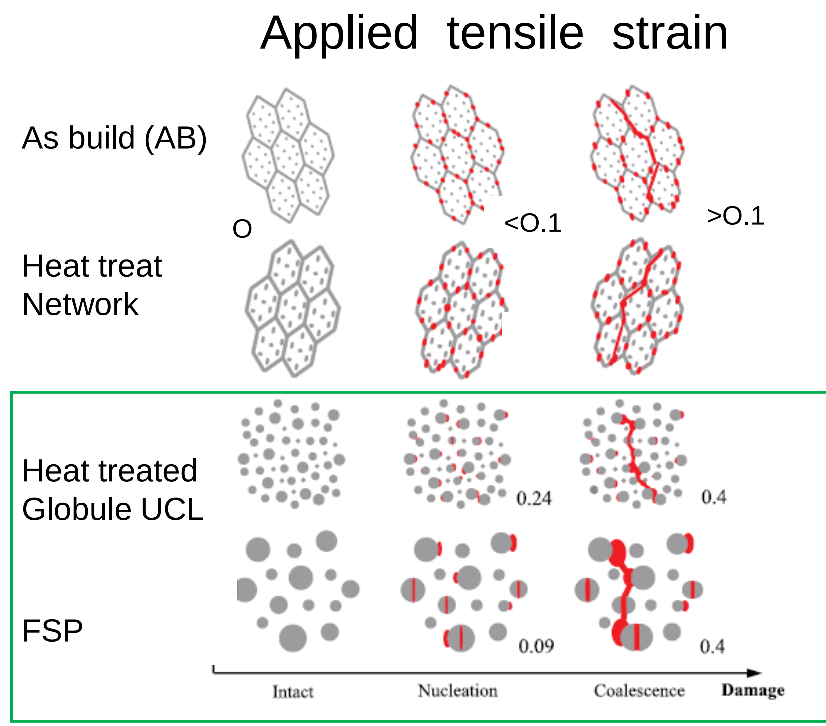

EMMC18

LongLifeAM RW project

(Zhao et al. MSEA 2019)

Is Phase Field

+ analytical tool able to provide

- → **the microstructure**
- → **the thermophysical properties**
- → **the mechanical properties σ_y**

?

→ **To be confident in Phase Field results:**

First predictions should be validated by experiments

Phase-Field model

AlSi10Mg simplified :Al-Si α-Al matrix + Si-diamond

Delahaye et al. Rice 2021

Fetni et al. Complas 2021

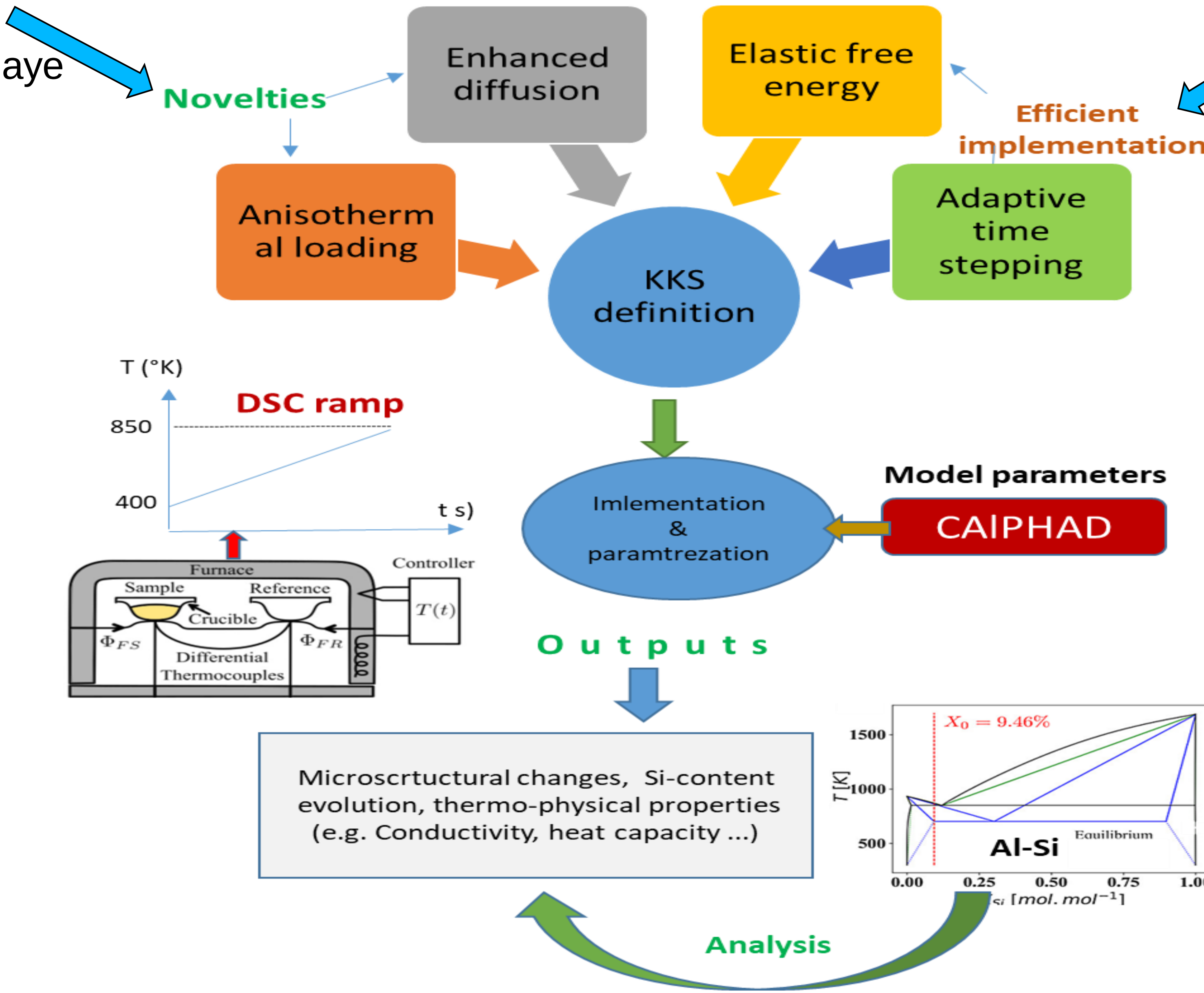

Uliege enhanced Kim Kim Suzuki “KKS” model

See

- S.G. Kim Physical Review E 60 (6) (1999) 12
- J.Z. Zhu, Acta Materialia 52 (2004)

Phase-Field model validation

2D simulation of a AB AlSi10Mg heated at a rate 20 K/min for DSC modelling

Governing equations:

Cahn Hilliard

$$\frac{\partial X_{Si}}{\partial t^*} = D^*\nabla^*.\left[\frac{f_{0_{X_{Si}\eta}}}{f_{0_{X_{Si}X_{Si}}}}\nabla^*\eta + \nabla^* X_{Si}\right]$$

Allen Cahn

$$\frac{\partial \eta}{\partial t^*} = -L^*\left(f_{0\ \eta}^* - \kappa^{*2}\nabla^{*2}\eta + e_{el_\eta}^*\right)$$

η 1 ➔ diamond Si phase
0 ➔ FCC Al phase

X_{si} molar fraction of Si

F_0 homogeneous free energy density

e_{el} elastic strain energy

K interface contribution

L interface kinetic coefficient

D diffusion coefficient

* Modified due to excess of vacancies

=> Fourier spectral method (FFT) with a semi-implicit form

$$\frac{\{X_{Si}\}_k^{n+1} - \{X_{Si}\}_k^{n}}{\Delta t} = D^* i\boldsymbol{k}.\left\{\frac{f_{0_{X_{Si}\eta}}}{f_{0_{X_{Si}X_{Si}}}}[i\boldsymbol{k}'\{\eta\}_{k'}^{n}]_r\right\}_k^n - D^* k^2\{X_{Si}\}_k^{n+1}$$

$$\frac{\{\eta\}_k^{n+1} - \{\eta\}_k^{n}}{\Delta t} = -L^*\left(\left\{f_{0\ \eta}^*\right\}_k^n + \kappa^{*2}k^2\{\eta\}_k^{n+1} + \{e_{el_\eta}\}_k^n\right)$$

Phase-Field enhanced KKS model

2D simulation of a Si precipitate "wall" representative of AB microstructure

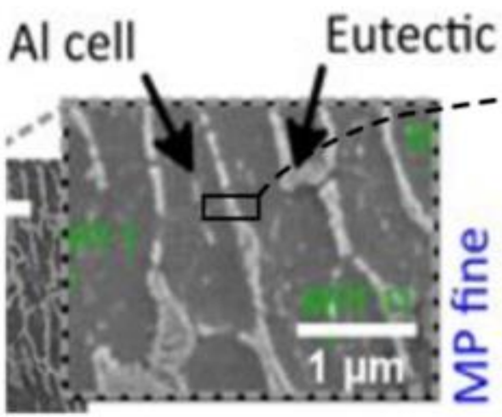

(a)

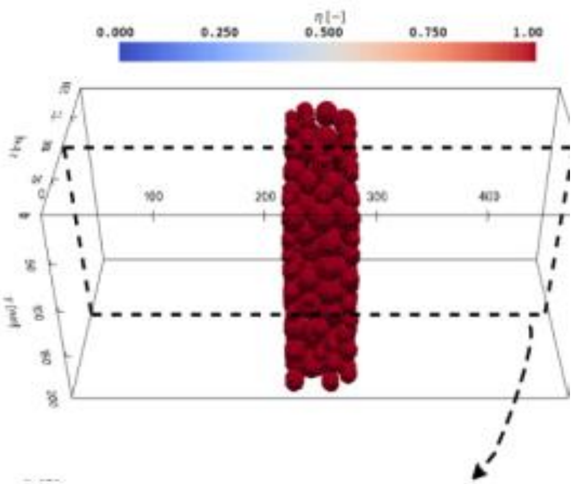

(b)

Loading: heating rate 20 K/min

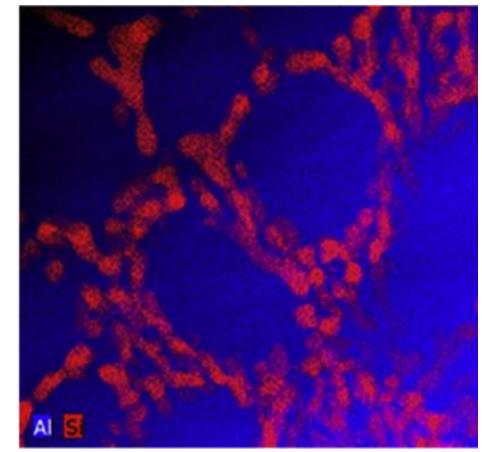

X.P. Li et al., Acta Mater. **95** (2015), 74-82

1st case **L** (interface mobility coefficient) bounded by a fct of tp°)

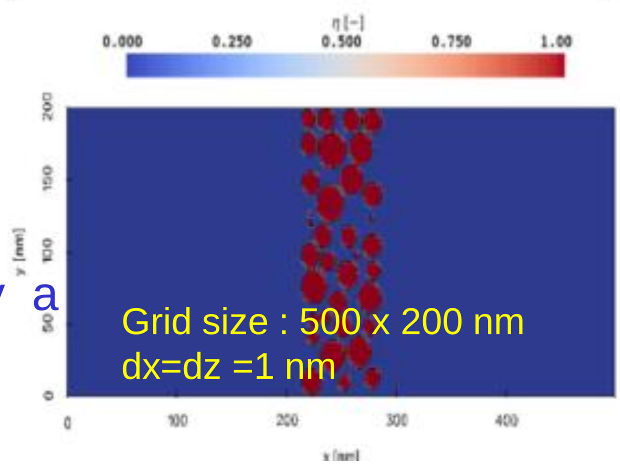

See Delahaye et. al ICAA2020 conf and ESAFORM 2021 (Orbi pdf)

Initial Si particle : ϕ=20 nm

2nd case **L** not bounded

L ↓: mitcrostr. evolution interface controlled, low transformation kinetic.

L ↑: diffusion-controlled, high kinetic for Tp° ↑

Eutectic network

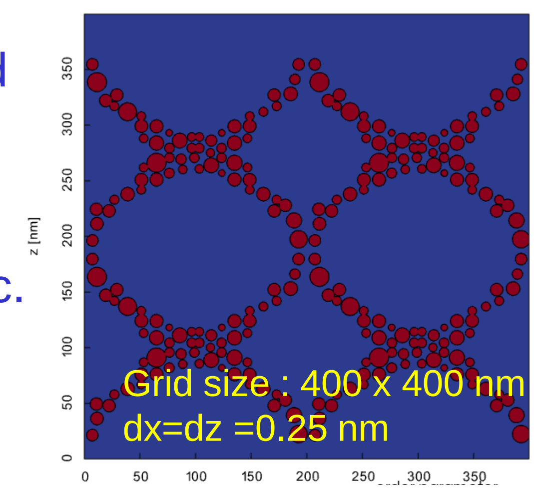

EMMC18 **Representative network of eutectic rich Si "walls" of AB**

Phase-Field simulations

2D simulation of a Si precipitate wall heating rate 20 K/min // DSC 1st run

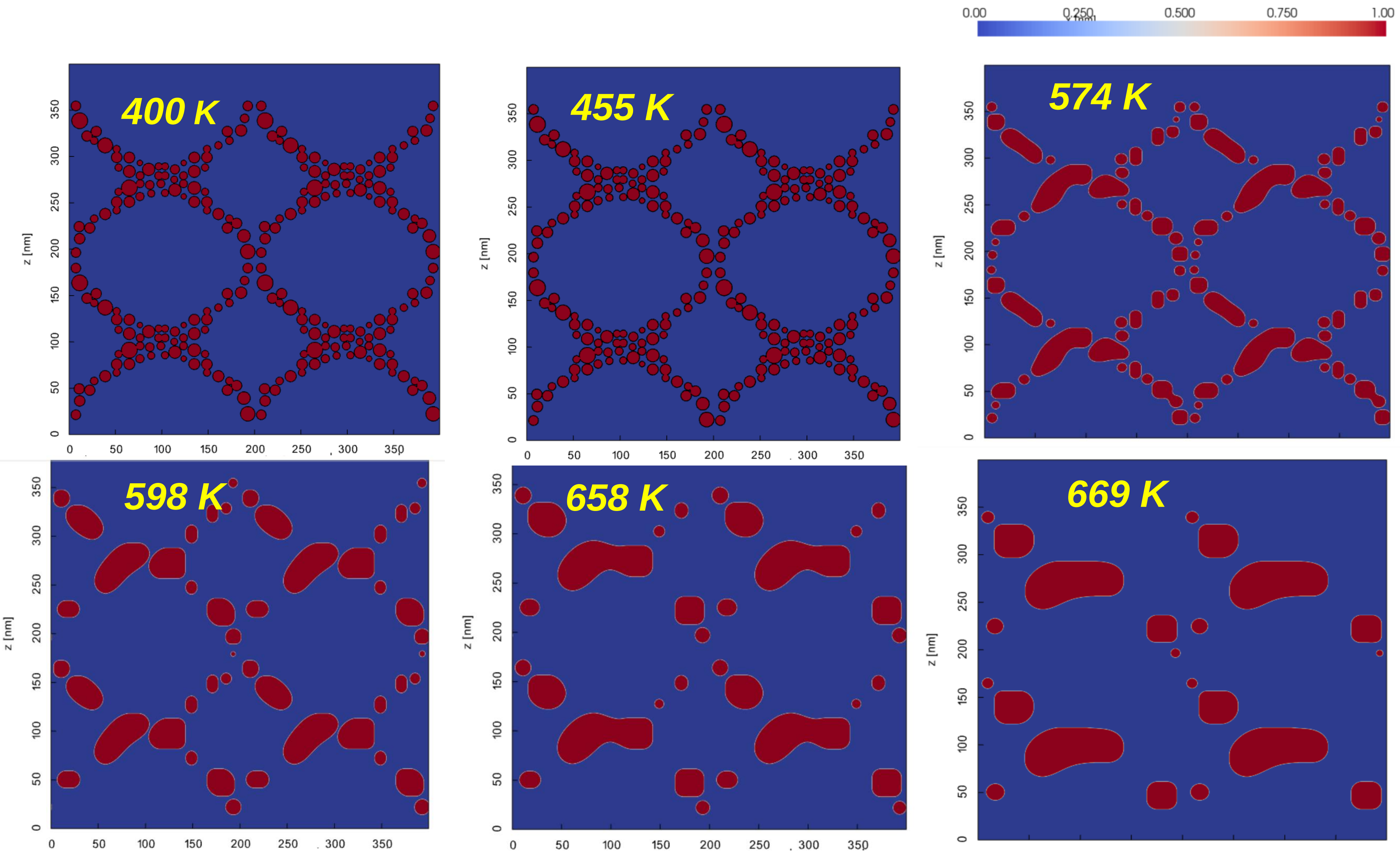

Phase-Field result versus experiment

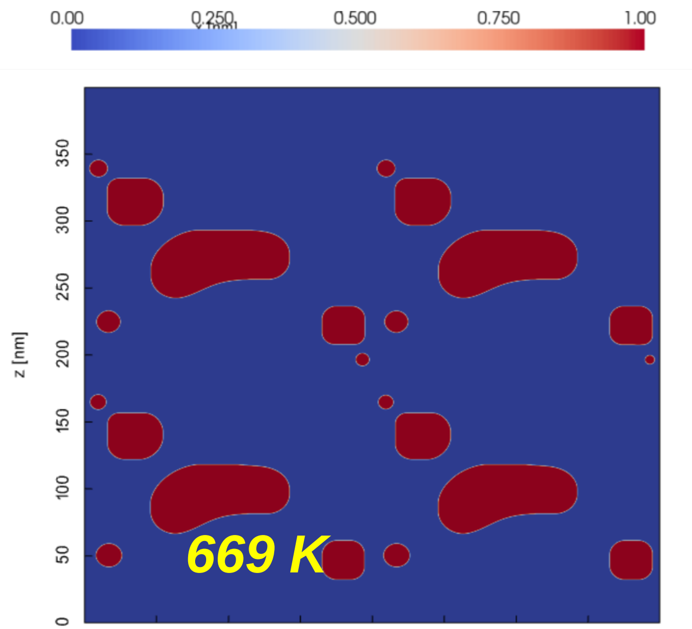

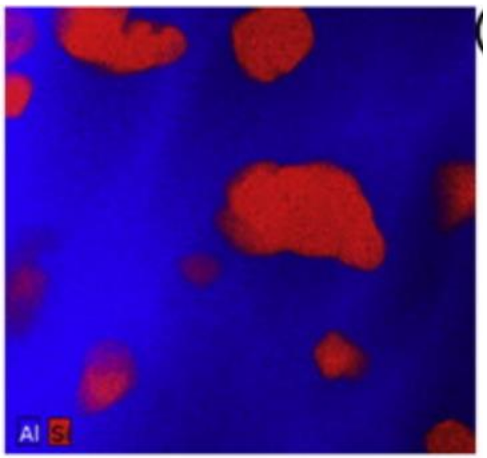

STEM-EDX maps of the Al and Si distribution in the Al–12Si alloy, isothermal Loading at 500 °C for 4h

X.P. Li et al., Acta Mater. **95** (2015), 74-82

⇒ Evidence of the coalescence and growth phenomena

⇒ rich-Si eutectic network diappears

Delahaye et al.
Rice 2021 (Orbi Uliege)

Link with DSC capacity and conductivity curves ongoing

Delahaye et al article, submitted ActaMat

Analytical tools based on microstructure ➔ Prediction of mechanical properties For α-Al matrix, Si particles

Analytical tools to compute macroscopic yield strength : σ_y

$$\sigma_y = \sigma_i + \sigma_{ss} + \sigma_p + \sigma_d$$

Dislocation hardening

σ_i : Intrisic yield strength: pure aluminium

σ_{ss} : Solid solution strengthening

σ_p : Precipitation strengthening contribution

In AB effect of
Build platform
Tp° 35°, 165°, 200°C
Eutectic walls and cells

In AB + FSP
Si particles, *ongoing*

O. Bouaziz and P. Buessler. Mechanical behaviour of multiphase materials : an intermediate mixture law without fitting parameter Rev. Met. Paris 99.1 (Jan. 2002)

O. R. Myhr, Grong, and S. J. Andersen. Modelling of the age hardening behaviour of AlMgSi alloys". Acta Materialia 49.1 (2001)

Analytical tools based on microstructure
➔Prediction of mechanical properties
For As Built 35°C, 165°C, 200°C

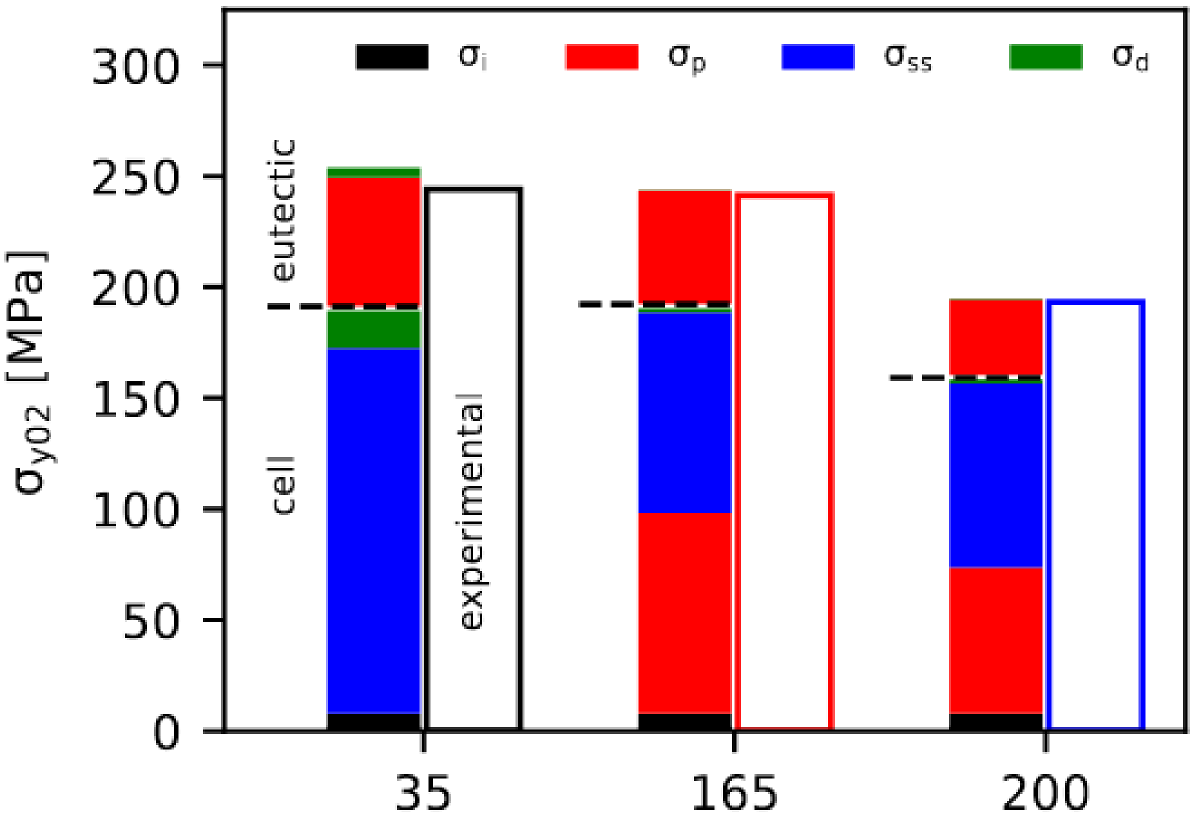

σ_i Al yield strength
σ_{ss} Solid Solution
σ_d Si particles
σ_p particles strengthening in eutectic or cell

+ isomechanical work between the cells and the eutectic

→ the important effect of the solid solution in the cells.

→ If temperature↑:

Precipitation & coarsening
Eutectic ↓

Image and XRD analysis = input of analytical tools ;
Experimental yield stress from tensile tests

Is RVE model able to provide

→ Macroscopic σ-ε AlSi10Mg for different microstructures
→ Local strain and stress fields
→ Damage mechanism

?

To be confident RVE results :

First prediction validated by experiment

AB + FSP → Matrix + Particles → RVE

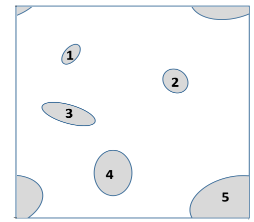

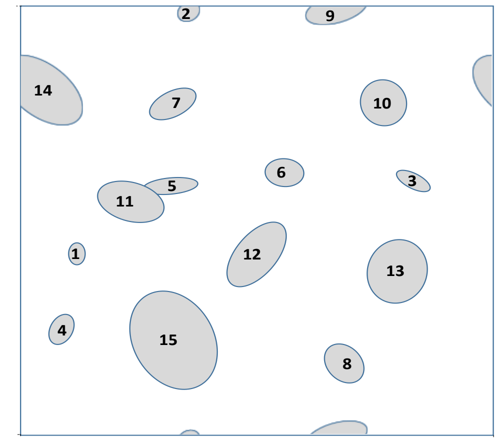

2D or 3D → 2.5D

Representative Size → 10 particles

Mesh density → medium

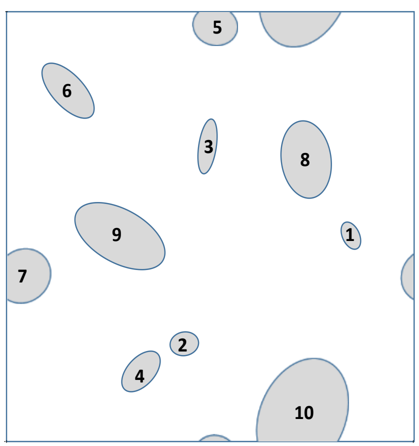

Strong strength ratio
Si particle
α-Al matrix

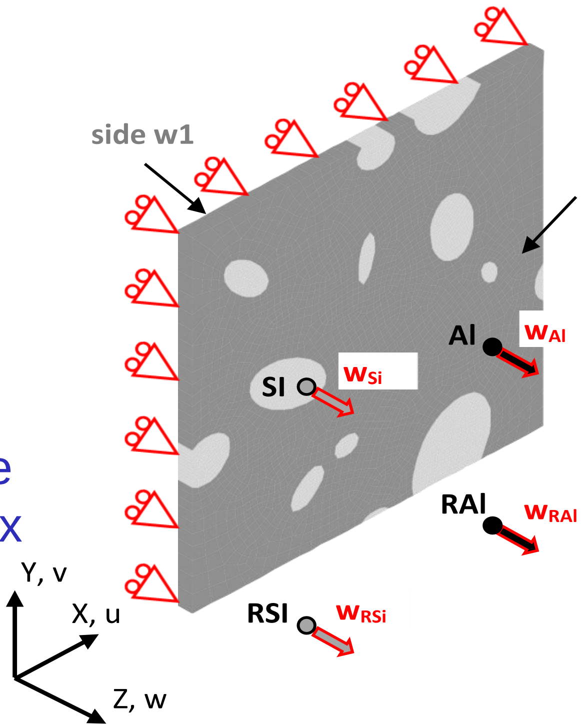

Target: representativity of a macro tensile test in Y dir.

Macro level : $\varepsilon_X \approx \varepsilon_Z$ isotropic material

Local level: strength in z dir
Identical for all particles
Interface: Cohesive elements

Bouffioux et al. 2022

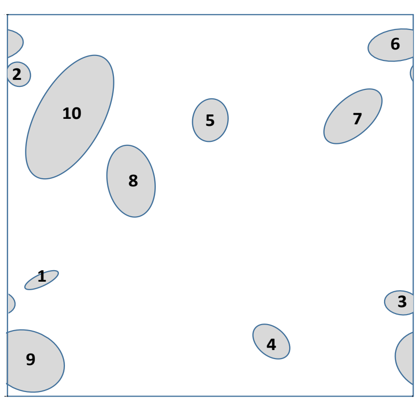

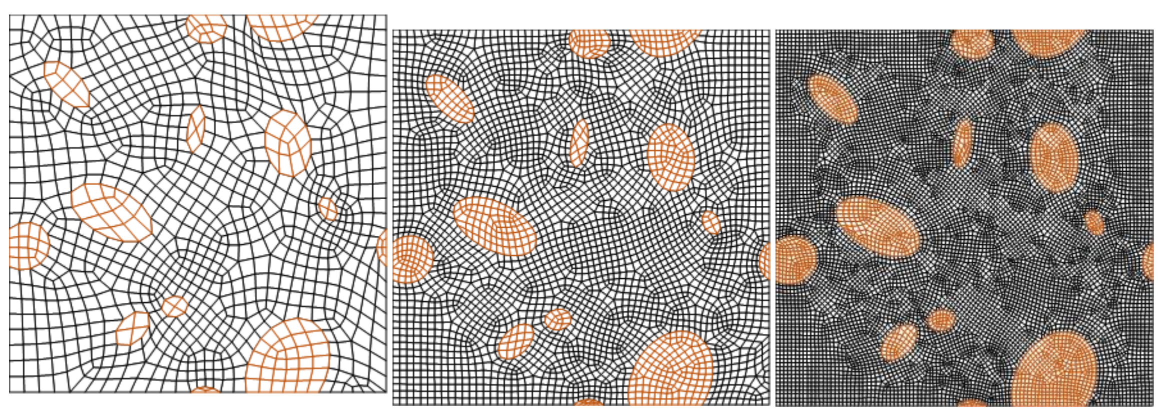

σ-ε curve of each components?

σ-ε curves of α-Al matrix, Si particles

AlSi10Mg AB + FSP = α-Al matrix + Si particles

Si : literature + nanoindentation of big particles (young modulus)

α-Al matrix: nano- indentation of α-Al matrix

and interactions with PF + analytical formulas

Tran Song Hoang et. al submitted to Int.Journal of Mec.Sciences 2022

+ Dedry et al. Proc. ESAFORM 2021 (PoPuPs)

→ Possibility to validate our approach

→ Possibility to go toward virtual material state

α-Al matrix caracterisation by nanoindentations

1 point ($\varepsilon_{r,\theta}$, $\sigma_{r,\theta}$) for each indenter characterized by its angle α

- **Nanoindentation curves**

→ $F = C.\ h^2$ with F: normal force, h: penetration depth, C: constant

→ $$\frac{1}{E^*} = \frac{1-\nu^2}{E} + \frac{1-{\nu_i}^2}{E_i}$$ with E*: reduced modulus of the curve

- **K.L. Johnson (J. Mech. Phys. Solids, 1970)** → $\varepsilon_{r,\theta} = K\ .\ cotan\ (\theta)$

the characteristic strain $\varepsilon_{r,\theta}$

θ: angle of the equivalent cone, K = 0,105 (Bucaille, Acta Mat. 51, 2003)

→ $$\theta = arctan\left(\sqrt{\frac{3.\sqrt{3}}{\pi}}.\ tan(\alpha)\right)$$ with α: angle of indenter

- **Dao's method (Acta Mat. 49, 2001) + Bucaille method (Acta Mat. 51, 2003)**

$$\Pi_{1\theta} = \frac{C_\theta}{\sigma_{r,\theta}} = tan^2(\theta).\left\{P1.\left[ln\left(\frac{E^*}{\sigma_{r,\theta}}\right)\right]^3 + P2.\left[ln\left(\frac{E^*}{\sigma_{r,\theta}}\right)\right]^2 + P3.\left[ln\left(\frac{E^*}{\sigma_{r,\theta}}\right)\right] + P4\right\}$$

the characteristic stress $\sigma_{r,\theta}$

P1	P2	P3	P4
0.02552	- 0.72526	6.34493	- 6.47458

α-Al matrix caracterisation by nanoindentations

Indentations on grids with 3 different indenters→ lowest curves for matrix

→ Swift or Voce hardening law fitting

infinite solution if σ_y not defined

→ σ_y from macro tensile macro

→ Ok high ratio Si/ α-Al strength & low fraction of Si particles (*Tran et. Al 2022*)

Berkovich

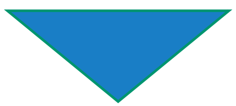

θ_1

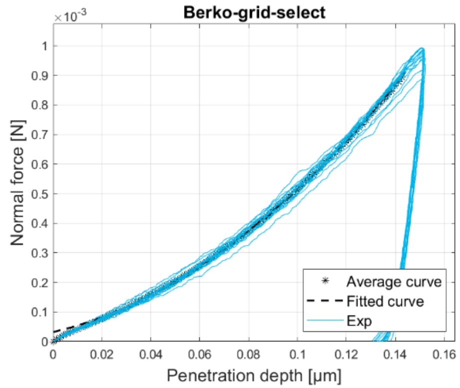

v

50°

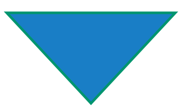

θ_2

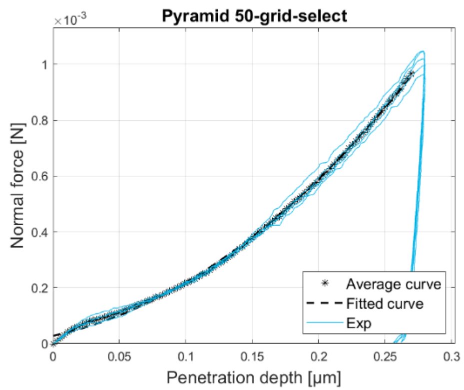

v

Cube corner

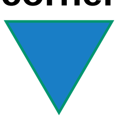

θ_3

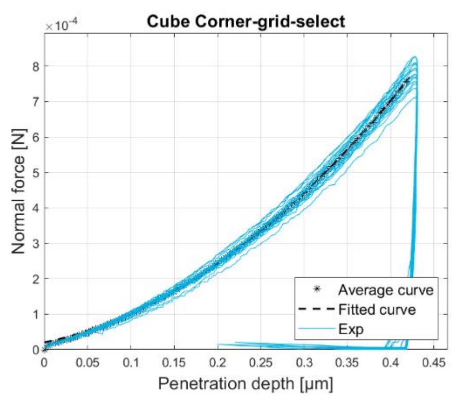

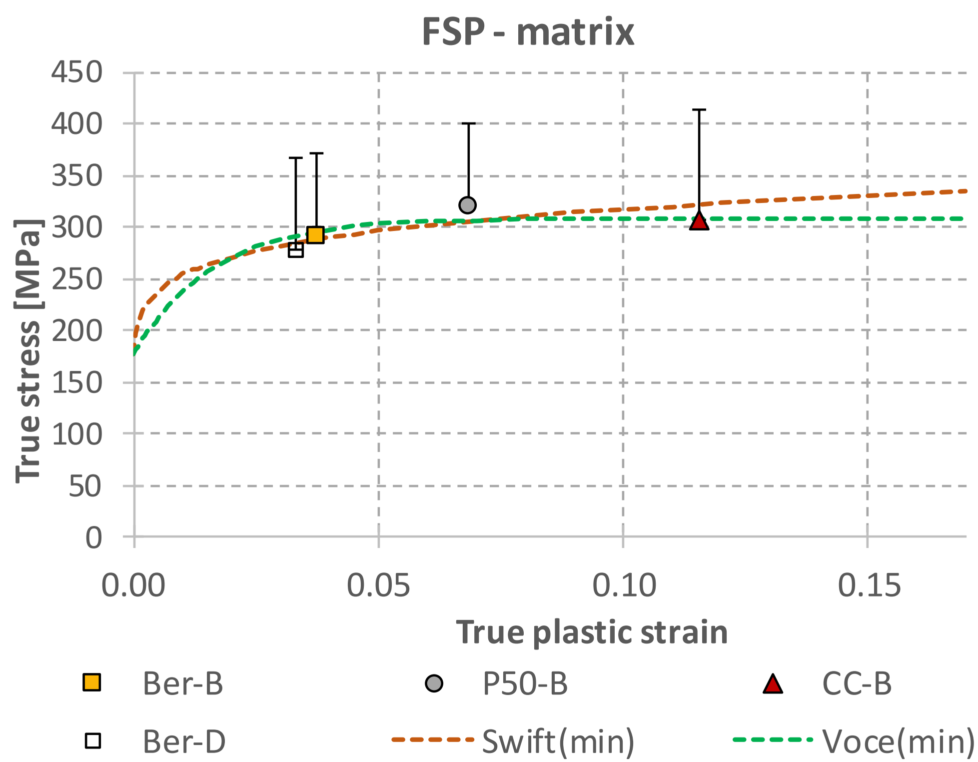

O. Dedry, C. Bouffioux, H;S.Tran, J. Macías, A.M. Habraken, A. Mertens, (2021) ESAFORM proceedings

Macroscopic σ-ε computed from RVE

Tensile test in y direction

Experimental validation

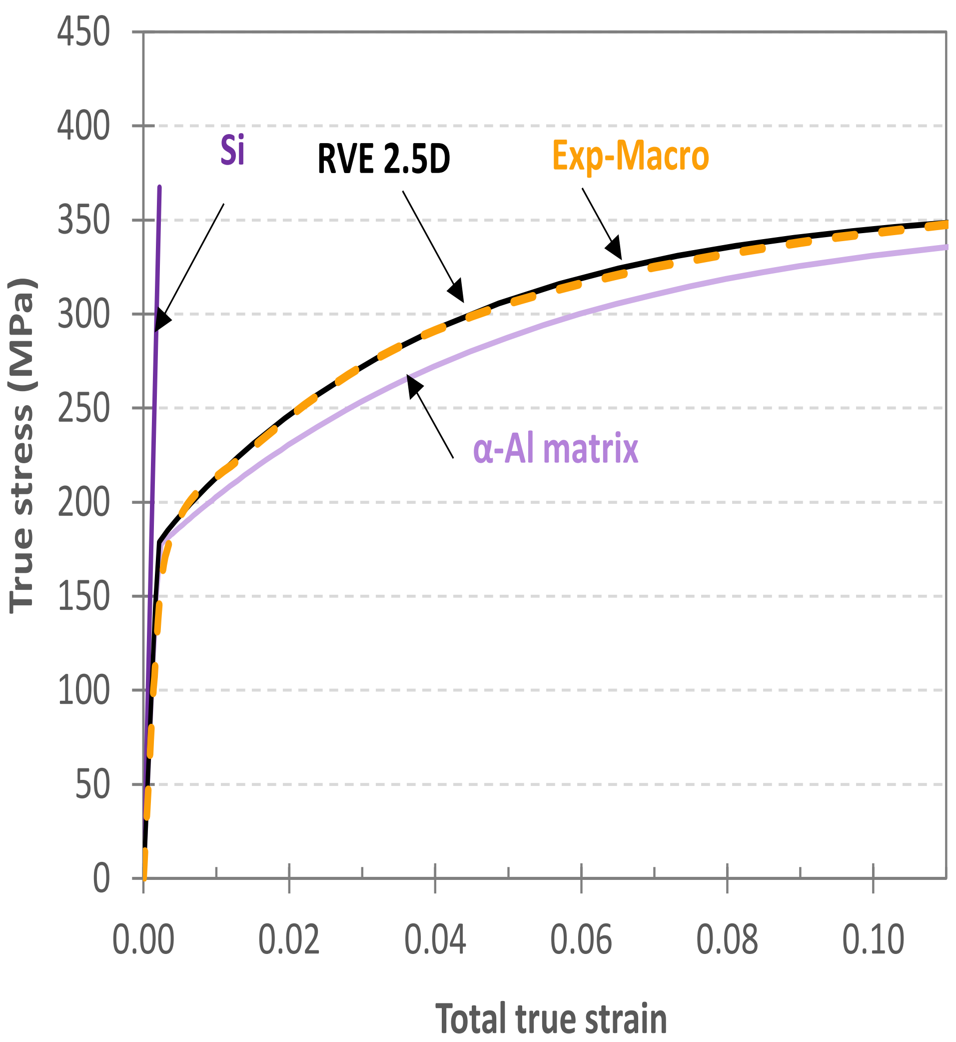

Effect of z boundary condition

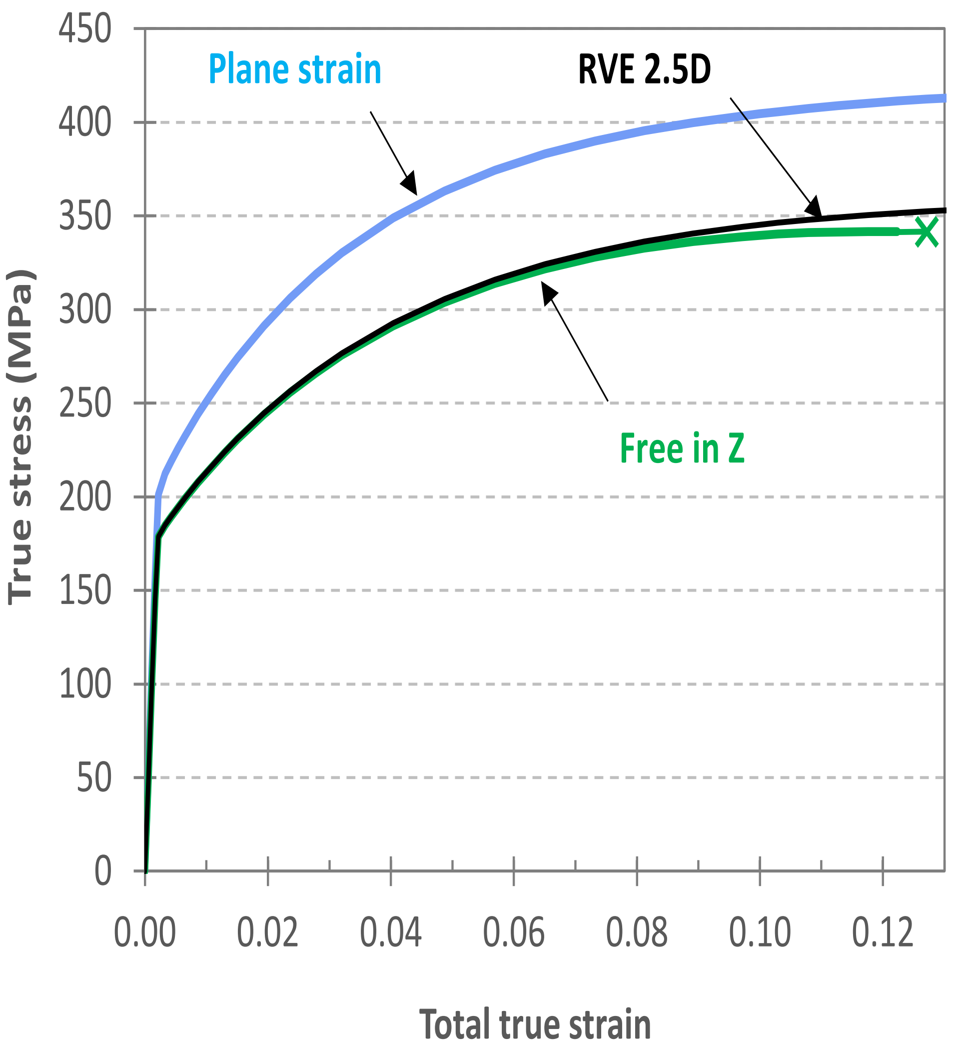

Local stress field

Periodic conditions in XY plane
Force applied in y

Effect of Boundary conditions in z direction

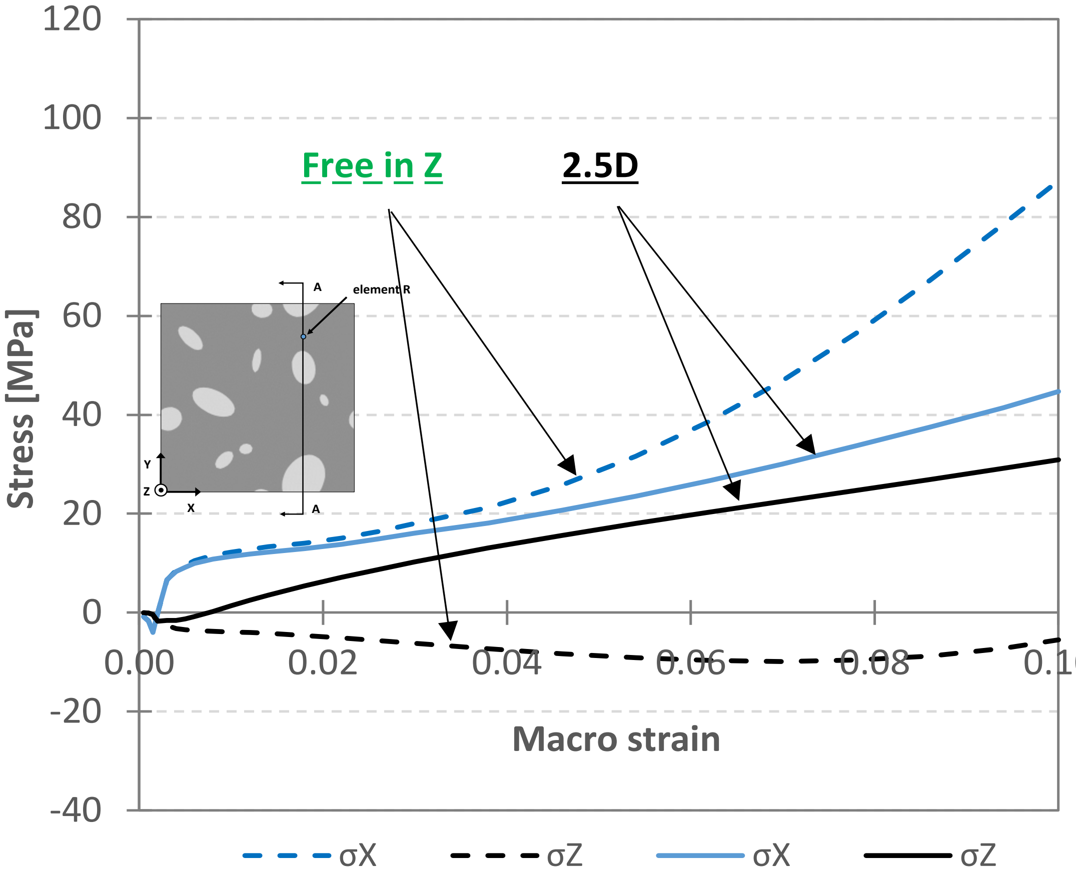

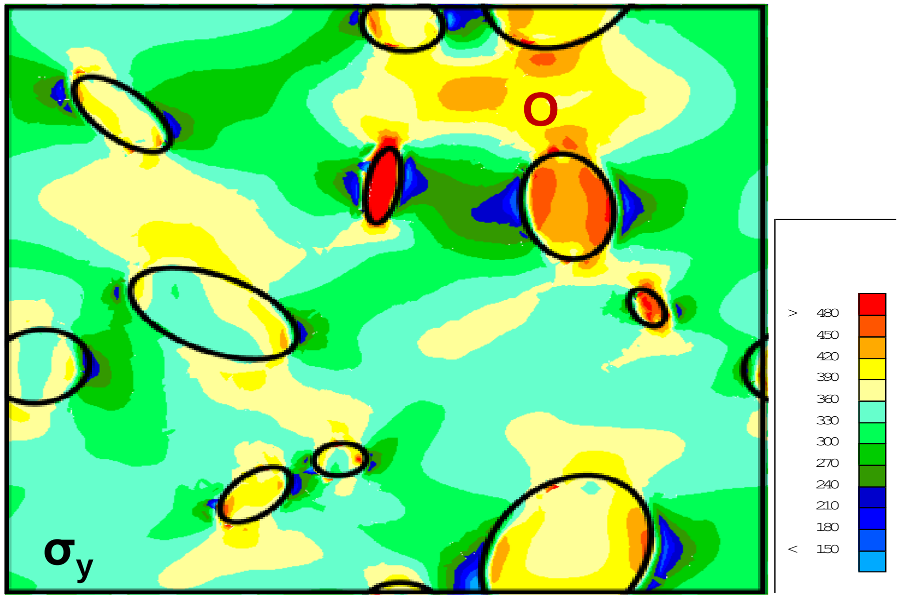

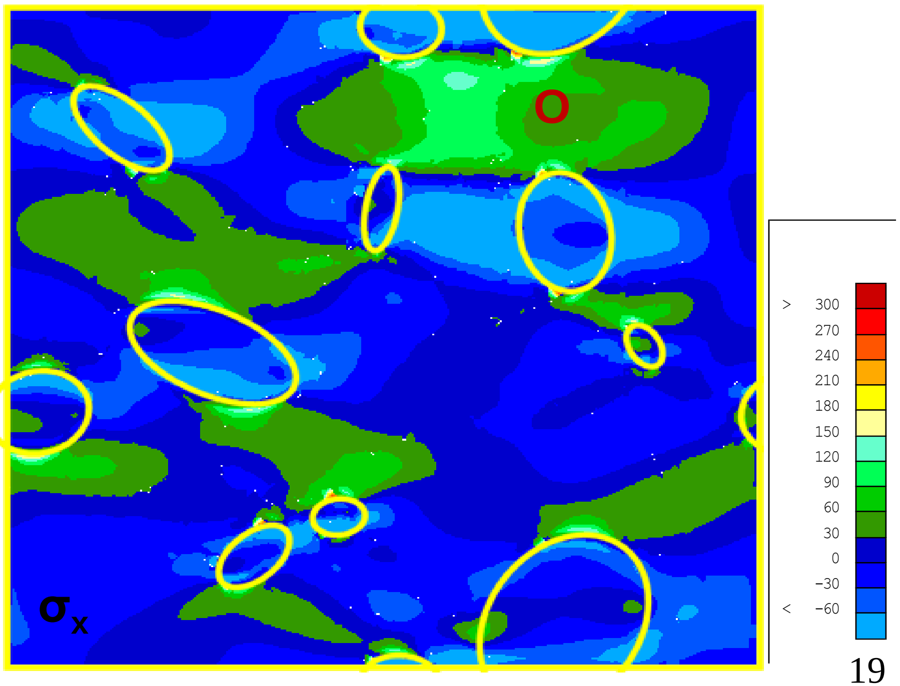

Sensitivity of local max σ_y to mesh & RVE size

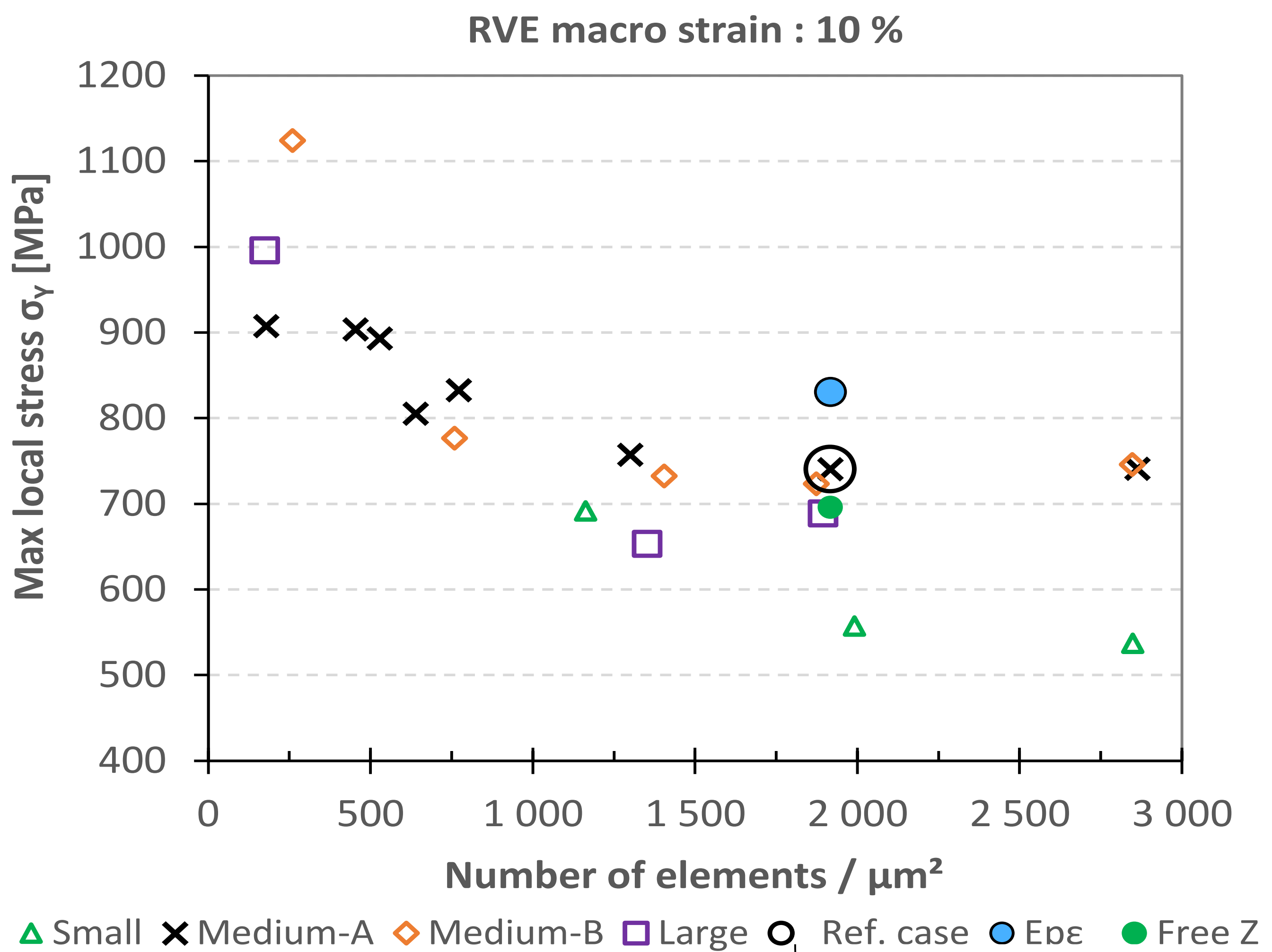

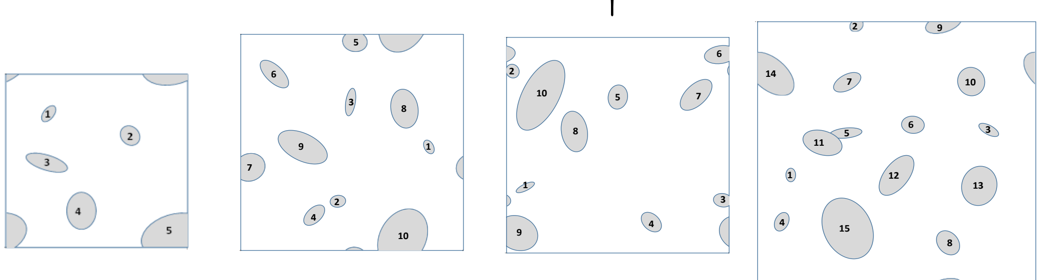

2.5D

Plane strain

For Medium-A RVE Effect of boundary condition

No macro stress however effect of strength heterogeneity (3D law 1 element layer mesh)

Damage mechanism in static loading → Cohesive interface elements

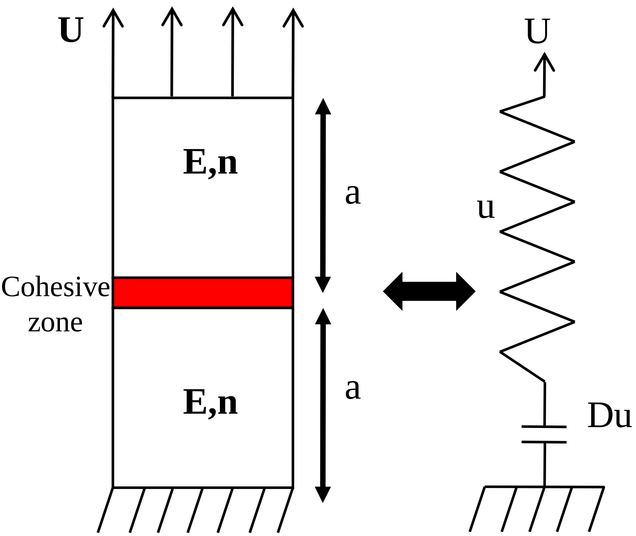

Uniaxial problem to illustrate the jump displacement

$$
T = \begin{cases} \dfrac{\sigma_{max}}{\delta_0}\Delta u & \text{if } \Delta u < \delta_0 \\ \sigma_{max}\dfrac{\delta_c - \Delta u}{\delta_c - \delta_0} & \text{if } \delta_0 \le \Delta u \le \delta_c \\ 0 & \text{if } \Delta u > \delta_c \end{cases}
$$

Bilinear law

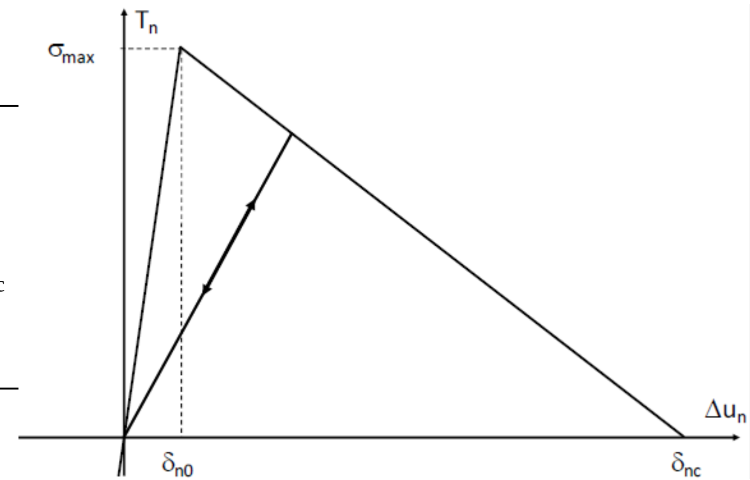

Traction separation law

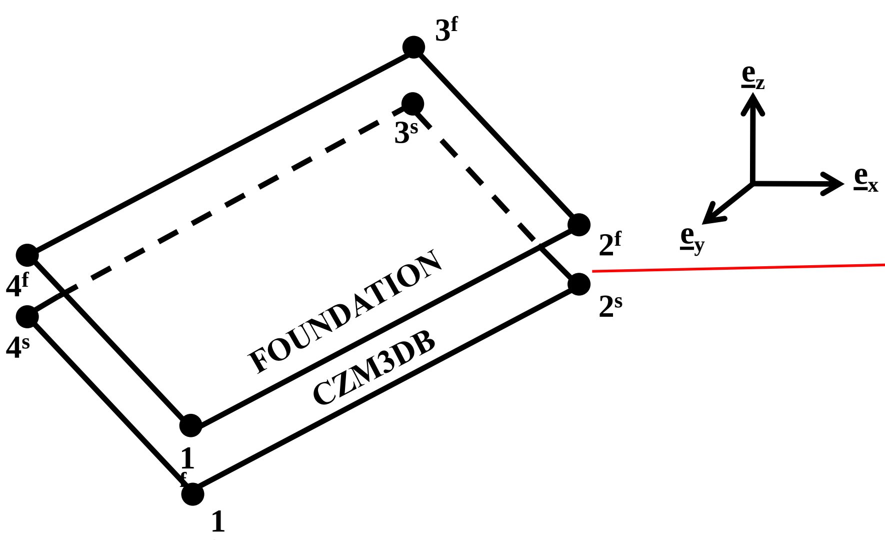

Three-dimensional cohesive zone

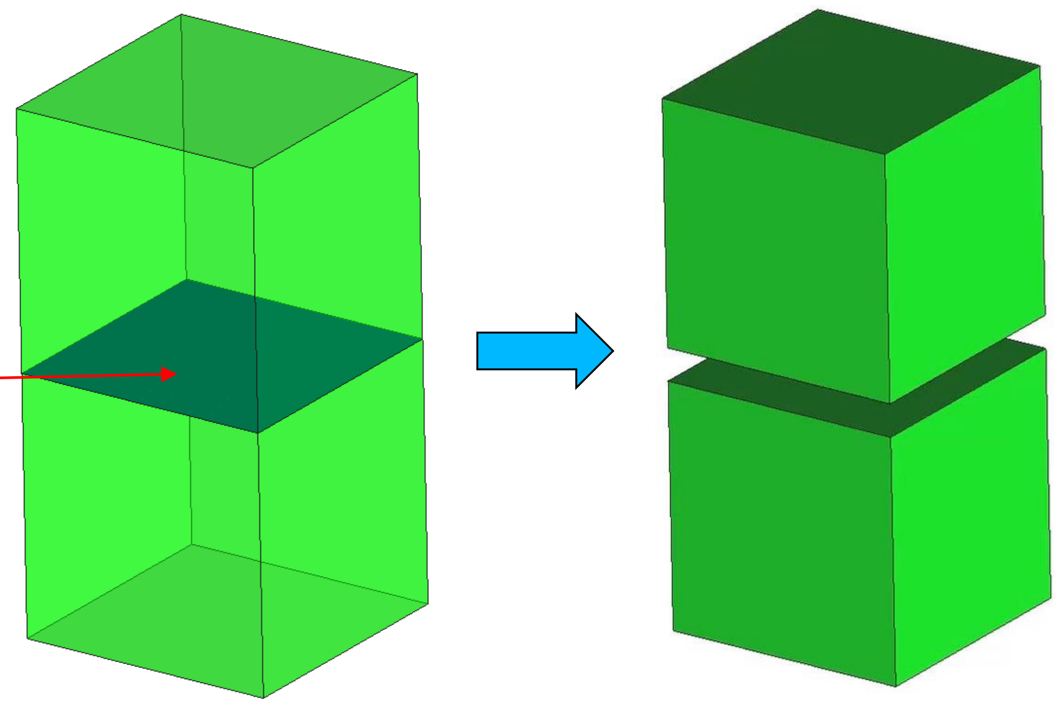

Cohesive zone modelling

Microstructure of AlSi10Mg after FSP

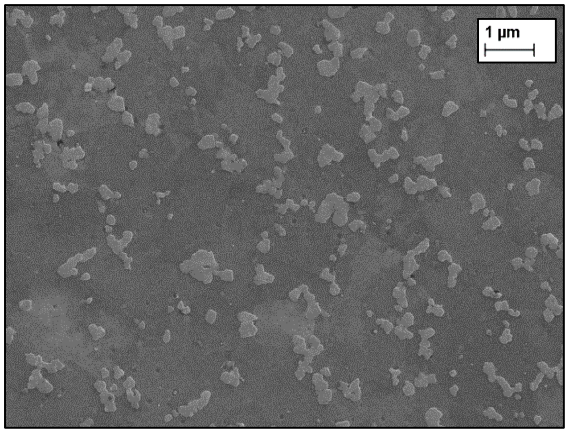

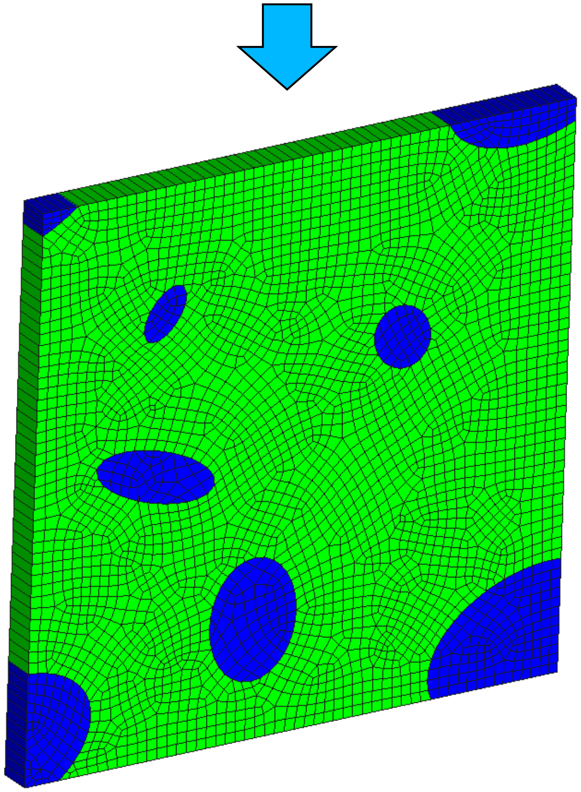

Finite element model of the Representative Volume Element (RVE)

σ_{max}	δ_{n0}	δ_{nc}	τ_{max}	δ_{t0}	δ_{tc}
550	5.5E-6	6E-6	550.	5.5E-6	6E-6

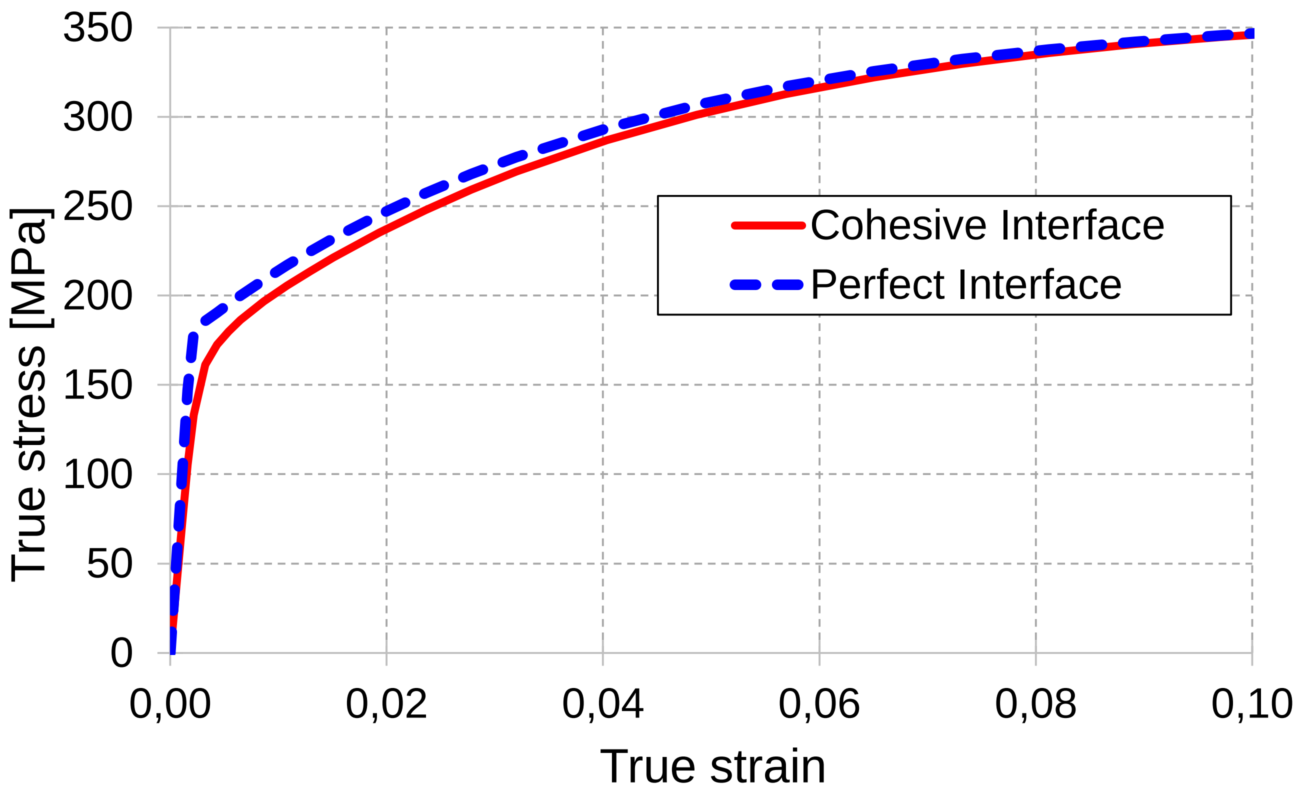

Sensitivity of local field assumption at macro strain 0.1

Perfect Interfaces

Cohesive Interfaces

Equivalent Strain

Stress-YY

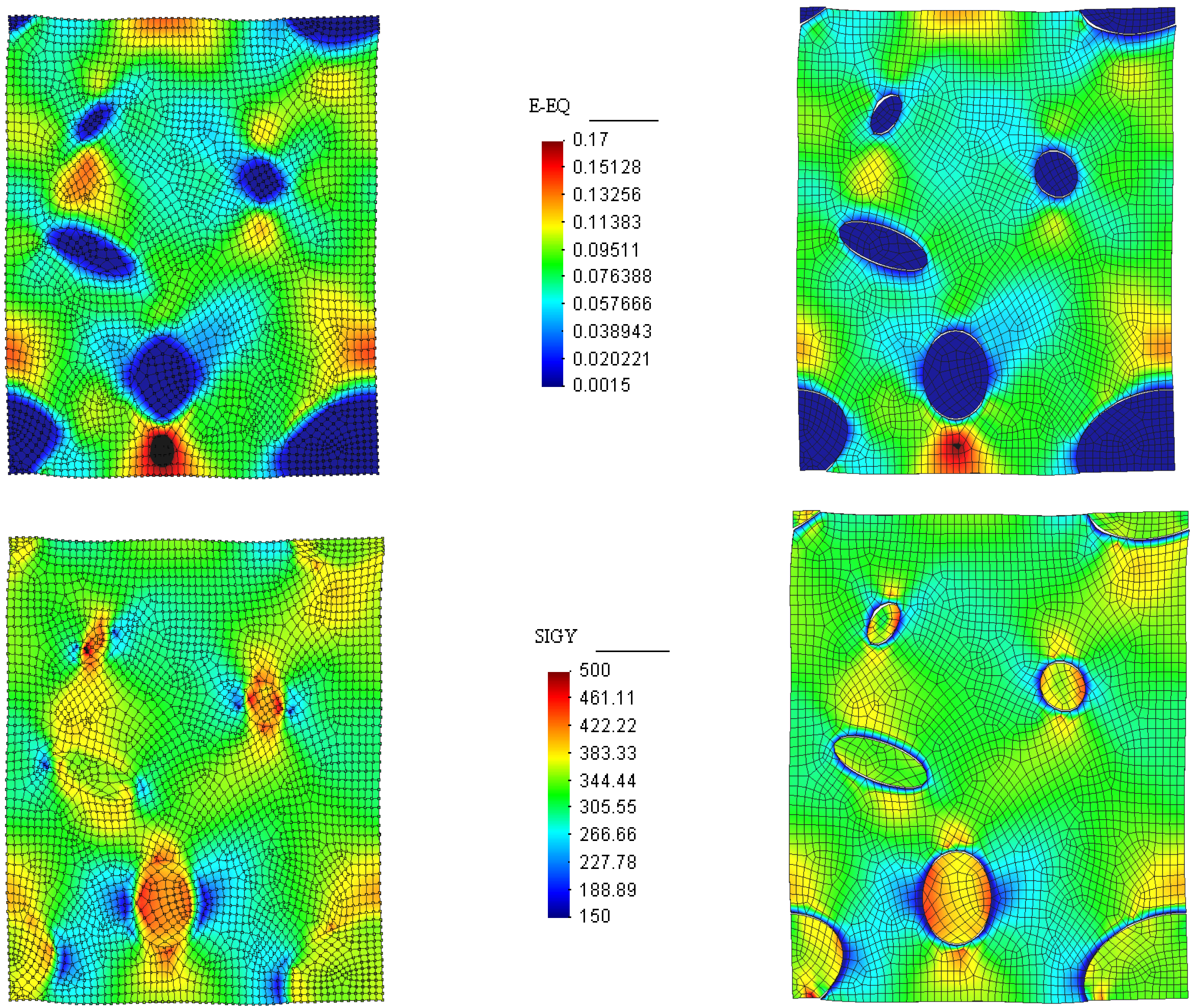

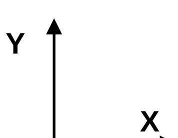

Toward numerically optimize post treatments of AB (TT, FSP) ?

2.5D RVE developed → validated macro stress strain tensile curve ✓
→ local stress and strain fields available ✓
→ damage mechanism in static loading *ongoing*
(Input data from experiments or Phase Field approach)

Phase field → microstructures predicted from Tp° history ✓
→ validated by 1rst run DSC curve ✓
+ microstructure evolution (EMMC18)

Analytical tools → validated mechanical properties
on AB 35°c, 165°C, 200°C ✓
(Input data from experiments, from PF *ongoing*)
→ validated thermophysical properties on AB 35°c ✓
(Input data PF, Delahaye et al. Rice 2021, ESAFORM 2021)

Next steps: *fatigue*
fatigue experimental campaign
RVE predictions via damage constitutive laws